

## Homogenization of Alloying Particles in Induction Crucible Furnaces

M. Ščepanskis, A. Jakovičs, B. Nacke

### Abstract

The present paper contains the result of the numerical modelling of the industrial process of the particle homogenization in induction crucible furnaces. The LES method is used to simulate the flow of liquid metal and the Lagrangian equation is used for particle tracking. The algorithm is implemented by means of the development of the *OpenFOAM* software code. The analysis of the numerical results allows us to conclude that big particles concentrate in a thin layer near the wall and the number of the particles in the layer is much bigger for the particles with low density. The homogenization of the particles with the density equal to the liquid density occurs more rapidly than the homogenization of the light particles because of different behaviour of the particles in the middle zone of the crucible near the wall. The physical model of the particle motion in this zone is presented in this paper.

### Introduction

The different alloying particles are mixed in a steel melt to increase some properties, such as strength, hardness, wear resistance and the others. The different chemical elements that are used as alloying admixtures and their densities are shown on the Tab. 1. The density of alloy steel ranges between  $7.75$  and  $8.05 \text{ g/cm}^3$  (it depends on the alloying constituents). Thus there are the admixtures with approximately equal and lighter densities than the steel density. The most of alloying elements are pure conductive, thus we can consider non-conductive particles.

Tab. 1. The densities of alloying element

Chemical element	Density, $\text{g/cm}^3$
Nickel (Ni)	8.908
Manganese (Mn)	7.21
Chromium (Cr)	7.19
Vanadium (V)	6.0
Silicon (Si)	2.3290
Boron (B)	2.08
Carbon (C)	1.8 - 2.1

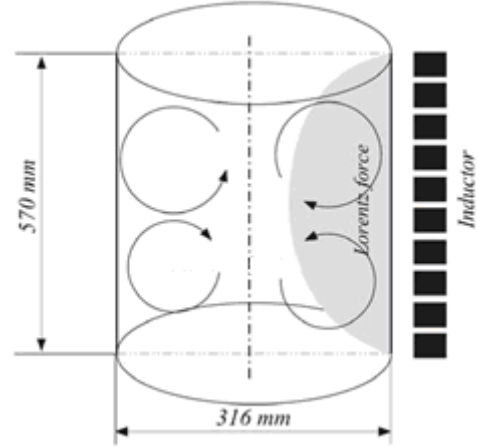
It is important to reach the homogeneous admixtures distribution to ensure a high quality of the alloy. At the same time it is very hard to investigate this process experimentally. Thus it is possible to choose the optimal parameters (such as the size of alloying particles, the time of mixing et al.) for industrial processes on the basis of the numerical simulation.

The simulation is carried out for the model of the cylindrical induction crucible furnace (ICF) which is typical object for inductive melting processes. The sketch of ICF is shown on the Fig. 1 and the sizes and the other parameters are shown on the Tab. 2.

The earlier results of the simulations were presented in [1], and the same method for the analysis of the process of homogenization is used in the present paper.

Tab. 1. The parameters of the laboratory scale ICF

Parameter	value
Inductor frequency	365 Hz
Inductor current	2000 A
Melt and inductor height	570 mm
Crucible radius	158 mm
Number of inductor turns	12



Fi

g. 1. The design of ICF with the sketch of the typical vortices of the mean flow

## 1. Model

### 1.1. The Model of the Liquid Flow and the Particle Tracking

Present model includes the flow and the particle motion simulation. The turbulent flow simulation is carried out using the Large Eddy Simulation (LES) method with the Smagorinsky subgrid viscosity model [2]. The flow is governed by electromagnetic (EM) force and thermal buoyancy force in the Boussinesq approximation [2]. The adiabatic and the convective thermal boundary conditions are considered.

The motion of the non-conductive particles can be described using the Lagrangian equation [3]:

$$\left(1 + \frac{C_A}{2} \frac{\rho_f}{\rho_p}\right) \cdot \frac{d\mathbf{u}_p}{dt} = C_D \cdot \mathbf{U} + \left(1 - \frac{\rho_f}{\rho_p}\right) \cdot \mathbf{g} - \frac{3}{4} \frac{1}{\rho_p} \mathbf{f}_{em} + \frac{\rho_f}{\rho_p} C_L \boldsymbol{\xi} + \left(1 + \frac{C_A}{2}\right) \cdot \frac{D\mathbf{u}_f}{Dt}, \quad (1)$$

where  $\mathbf{u}_p$  and  $\mathbf{u}_f$  are particle and liquid velocities respectively;  $\mathbf{U} = \mathbf{u}_f - \mathbf{u}_p$ ;  $\rho_p$  and  $\rho_f$  are particle and liquid densities respectively;  $\mathbf{g}$  is free fall acceleration; vector  $\mathbf{f}_{em} = [\mathbf{j} \times \mathbf{B}]$  is the Lorentz force density;  $\mathbf{j}$  is current density;  $\mathbf{B}$  is magnetic field induction; vector  $\boldsymbol{\xi} = [\mathbf{U} \times [\nabla \times \mathbf{U}]]$  describes the lift force;  $D/Dt$  is material derivation;  $C_D$ ,  $C_L$  and  $C_A$  are drag, lift and acceleration coefficient respectively and depend on the Reynolds particle number  $Re_p = d \cdot U/\nu$ ,  $d$  is a particle diameter,  $\nu$  is kinematic viscosity,

$$C_D = \frac{18\nu}{d^2} \frac{\rho_f}{\rho_p} \cdot (1 + 0.15 \cdot Re_p^{0.687}). \quad (2)$$

Equation (1) take into account drag, buoyancy, EM, lift, acceleration and added mass forces.

We consider particle transport model with several assumptions made [1, 3]:

- the particle-particle interaction is negligible,
- all particles are rigid spheres,
- the particles do not affect the structure and the velocities of the flow,

- the particles can slide along the wall but can not stick to the wall (the processes of the surface diffusion and the deformation of the particle are not considered).

### 1. 2. The Model of the Particle Collision with the Wall

The basic Lagrangian algorithm for the simulation of solid particles is already implemented in *OpenFOAM*. But it does not simulate the collision of a particle with the wall in the case when the size of the particle is more than the size of a cell. The present model takes into account the size of the particle and moves it to the distance of the radius from the wall if it is closer. In this case the particle can slip by the wall [3].

## 2. The Results of the Simulation

The process of the homogenization of alloying particles is considered for about  $3 \cdot 10^4$  particles with the diameters 0.05, 0.1 and 0.2 mm and the densities  $\rho_p = \rho_f/1.5$  and  $\rho_p = \rho_f$ . The particles are input on a horizontal plane near the top surface of the crucible, such the initial position of the particles corresponds to the industrial case.

The process of homogenization take place between the zones of two eddies (Fig. 2 (a)); therefore the difference between the number of the particles in the zone of the upper eddy and the one in the zone of the lower eddy is analyzed. The results of simulation show that the radial and angular distributions of the particles in the crucible rapidly became homogeneous.

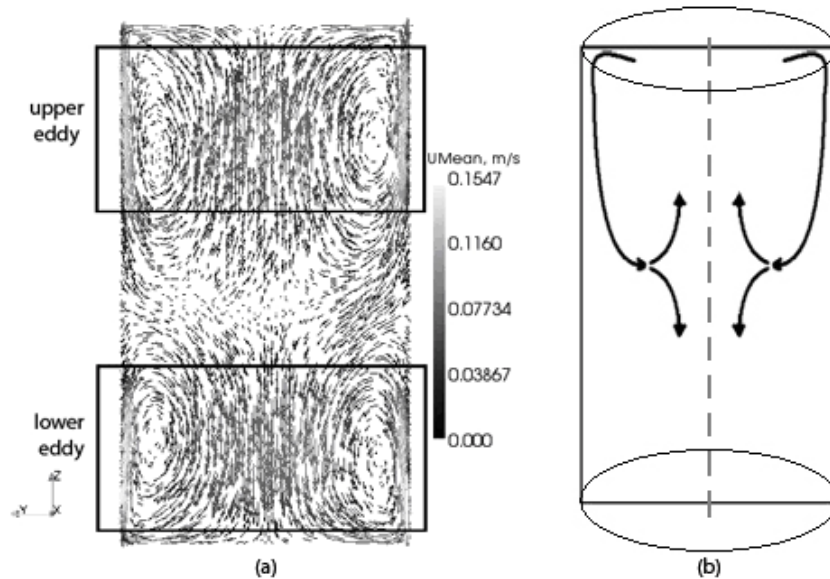


Fig. 2. (a) - the average flow velocity in the central vertical plane in ICF; (b) – a simplified scheme of the motion of the particle cloud in ICF

Fig. 2 (b) schematically shows the motion of the particles cloud. Initially all particles are going down from the initial position near the top surface through the zone of the upper eddy close to the wall to the middle part. Then the cloud of the particles separates: one part goes to the zone of the upper eddy and other part to the zone of the lower eddy. After that the particle exchange between two eddies decreases the difference between the

number of the particles in the zones of the upper and the lower eddies  $\Delta N$  with the lapse of time. Fig. 3 (a) and (c) shows the evolution of  $\Delta N$ , normalized with respect to the number of the particles in the both zones (in the frames on Fig. 2 (a))  $N$ , for the particles with a different diameter.

In the both cases the process of the homogenization is monotonous, but the particles with density  $\rho_p = \rho_f$  homogenizes more rapidly. Fig. 4 (a) shows that the most origin of such different homogenization velocities is the initial difference  $\delta$  that appears in the moment

when the particle cloud comes to the middle zone and separates in two clouds. The difference  $\delta$  increases significantly with increasing of the diameter of the particles.

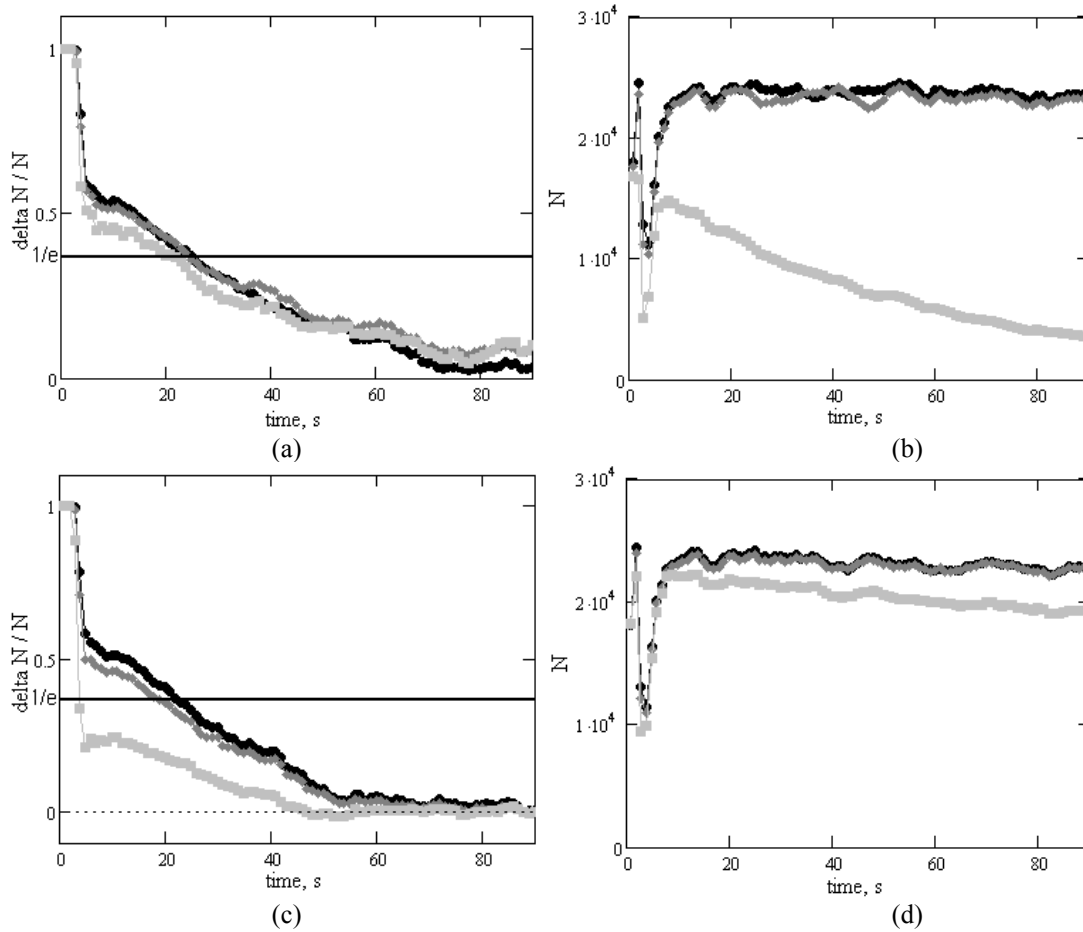


Fig. 3.  $\Delta N/N$  (a), (c) and  $N$  (b), (d) for particles with different densities: (a), (b) -  $\rho_p = \rho_f/1.5$ ; (c), (d) -  $\rho_p = \rho_f$ . The particles with different diameters:  $\bullet\bullet\bullet$  0.05 mm;  $\blacklozenge\blacklozenge\blacklozenge$  0.1 mm;  $\blacksquare\blacksquare\blacksquare$  0.2 mm

Fig. 4 (b) shows that the concentration of the big particles in the thin layer near the wall is increasing with the laps of time, the increasing is especially significant for the case of the light particles. The numerical simulation also shows that the number of the smaller particles in the layer is approximately constant value. It is the origin of the decreasing of  $N$  for big particles on Fig. 3 (b) and (d).

The results of the simulation show that the particles in the layer near the wall rapidly concentrate in the middle zone, where the EM force reaches the maximum magnitude. This fact corresponds to the experimental observation [4]. Thus the processes happened in this area significantly affect all process of the homogenization. So the physical model of the particle behaviour in the middle zone of the crucible near the wall is presented below.

### 3. The Discussion of the Results

The initial difference  $\delta$  (Fig. 4 (a)) and decreasing of  $N$  for big light particles (Fig. 3 (b)) can be explained with the physical model below.

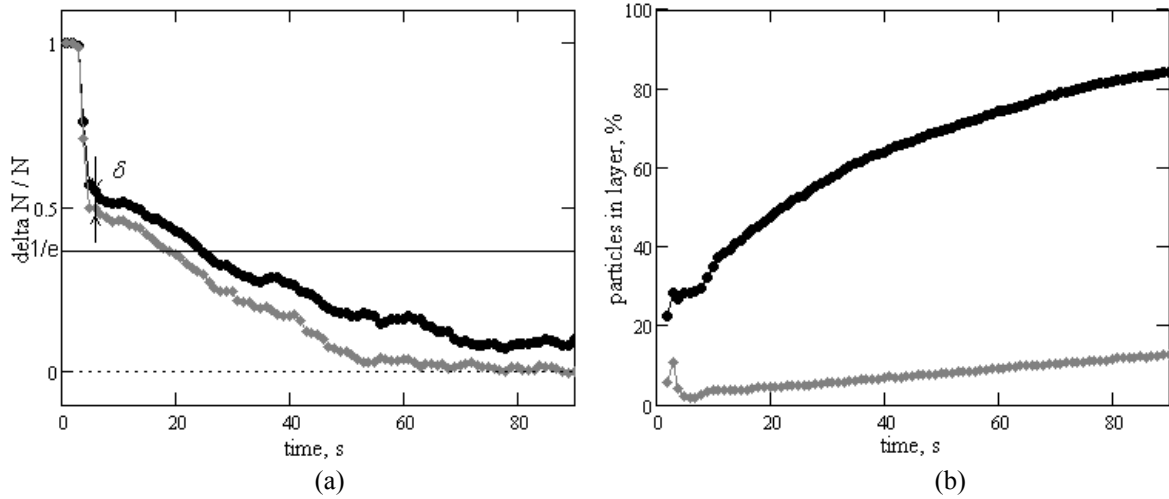


Fig. 4. (a) -  $\Delta N/N$  for particles with the diameter 0.1 mm; (b) – the number of the particles with the diameter 0.2 mm in the 4 mm thin layer near the wall. The particles with the different densities:  $\bullet\bullet\bullet \rho_p = \rho_f / 1.5$ ;  $\blacklozenge\blacklozenge\blacklozenge \rho_p = \rho_f$

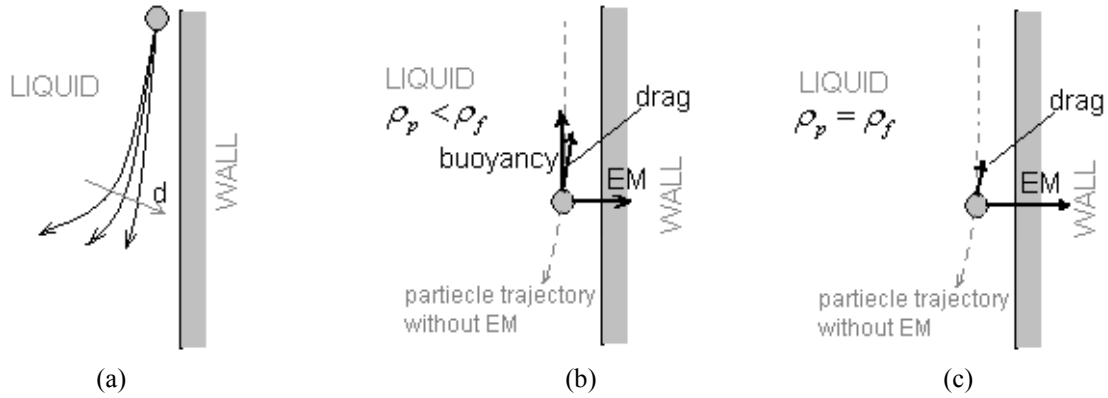


Fig. 5. (a) - simplified trajectories of the particle in the middle zone of the crucible near the wall for the cases with different diameters (arrow shows the increasing of diameter); (b), (c) – the directions of different forces of the big particle in the case  $\rho_p < \rho_f$  and  $\rho_p = \rho_f$  respectively

As it is described above the initial particle cloud comes to the middle zone by the wall. Let us consider the motion of the particle in the middle zone near the wall in this moment. The flow changes the direction in the considerable region (Fig. 2 (a)). Drag coefficient  $C_D$  is decreasing  $\sim d^{-2}$  with the increasing of the particle size (2). Thus drag force normalised with the mass in (1) is small for big particles and can not change their trajectories. With the increase of the particle size the direction of velocity of the particle becomes more vertical (Fig. 5 (a)).

Buoyancy and drag forces per mass unit are proportional to  $\rho_f / \rho_p$  (1). If we assume roughly that relative velocity  $U$  is equal for case  $\rho_p < \rho_f$  and  $\rho_p = \rho_f$ , then the forces in these two case are following:

$$\frac{(f_{drag}/m)_{\rho_f/\rho_p=S}}{(f_{drag}/m)_{\rho_f/\rho_p=1}} \cong S, \quad (f_{buoyancy}/m)_{\rho_f/\rho_p=S} = (1-S) \cdot \mathbf{g}, \quad \frac{(f_{em}/m)_{\rho_f/\rho_p=S}}{(f_{em}/m)_{\rho_f/\rho_p=1}} = 1.$$

Buoyancy and drag forces try to decrease the momentum and decelerate a light particle (Fig. 5 (b) and (c)). In the case  $\rho_p = \rho_f$  buoyancy force is equal to zero and only drag force try to stop the particle (Fig. 5 (c)). Thus in this case the deceleration of the particle is less efficiency and the big particles with greater probability come to the region of the lower eddy (Fig. 5 (b)). The EM force per mass unit is independent from  $\rho_f/\rho_p$  and pushes a particle to the wall. In the case  $\rho_p < \rho_f$  the particle can be efficiently decelerated and relatively large EM force lets it to stick to the wall in the middle zone (Fig. 5 (c)). This is the reason of the decreasing of  $N$  for big light particles (Fig. 3 (b)). With the increase of the particle size the drag coefficient is decreasing and consequently the probability of the particle sticking to the wall in the zone of intensive magnetic field is increasing. Thus this fact can explain the increase of  $\delta$  with the particles size increasing.

## Conclusions

The model of the homogenization of the particles in the ICF on the basis of the LES method for flow simulation and the Lagrangian equation for particle tracing are proposed.

The process of the homogenization is monotonous, but the particles with the density  $\rho_p = \rho_f$  homogenizes more rapidly than in the case  $\rho_p < \rho_f$ . The most origin of the difference in homogenization times in these cases in the initial difference  $\delta$  (Fig. 4 (a)).  $\delta$  significantly increases with the increasing of the size of particles.

The bigger particles concentrates in the middle zone of the crucible near the wall and the number of particles in this region significantly increases for the case  $\rho_p < \rho_f$  with the laps of time and reach 80% in 70 s for the particles with density  $\rho_p = \rho_f/1.5$ .

The processes in the middle zone of the crucible near the wall significantly affect the common process of the homogenization of the particles in the ICF and can explain the phenomena described above.

## References

- [1] Ščepanskis, M., Jakovičs, A., Nacke, B., Baake, E.: *The simulation of the behaviour of alloying admixture particles in the induction crucible furnaces*. Proceedings of the International Symposium on Heating by Electromagnetic Sources, Padua, 2010, pp. 3-10.
- [2] Kirpo, M.: *Modeling of turbulence properties and particle transport in recirculated flows (PhD thesis)*. University of Latvia, Faculty of Physics and Mathematics, Department of Physics, Riga, 2009.
- [3] Ščepanskis, M., Jakovičs, A., Nacke, B.: *The simulation of the motion of solid particles in the turbulent flow of induction crucible furnaces*. Proceedings of the V European Conference on Computational Fluid Dynamics, Lisbon, 2010.
- [4] Higuchi, M., Amabai, H., Shimasaki, S., Kamata, C., Teshigawara, S., Taniguchi, S.: *Electromagnetic separation of inclusions from molten copper by alternating electromagnetic field*. Proceedings of the VI International Conference on Electromagnetic Processing of Materials, Dresden, 2009, pp.86-89.

## Authors

Ščepanskis, Mihails  
 Prof. Dr.-Phys. Jakovičs, Andris  
 Laboratory for Mathematical Modelling  
 of Environmental and Technological Processes  
 University of Latvia  
 Zellu str. 8  
 LV-1002 Riga, Latvia  
 E-mail: Mihails.Scepanskis@lu.lv  
 E-mail: Andris.Jakovics@lu.lv

Prof. Dr.-Ing. Nacke, Bernard  
 Institute of Electrotechnology  
 Leibniz University of Hannover  
 Wilhelm-Busch-Str. 4  
 D-30167 Hannover, Germany  
 E-mail: Nacke@etp.uni-hannover.de